Quatsomes: Vesicles Formed by Self-Assembly of Sterols and Quaternary Ammonium Surfactants

ARTICLE *in* LANGMUIR · MAY 2013

Impact Factor: 4.46 · DOI: 10.1021/la4003803 · Source: PubMed

Langmuir

Article

pubs.acs.org/Langmuir

Quatsomes: Vesicles Formed by Self-Assembly of Sterols and Quaternary Ammonium Surfactants

Lidia Ferrer-Tasies,[†,‡,⊥] Evelyn Moreno-Calvo,[†,‡,⊥] Mary Cano-Sarabia,[†,‡] Marcel Aguilella-Arzo,[§] Angelina Angelova,[∥] Sylviane Lesieur,[∥] Susagna Ricart,[†] Jordi Faraudo,*[,†] Nora Ventosa,*[,†,‡] and Jaume Veciana[†,‡]

[†]Institut de Ciència de Materials de Barcelona (ICMAB-CSIC), Esfera UAB; Campus UAB s/n; E-08193 Cerdanyola del Vallès, Spain

[‡]CIBER de Bioingeniería, Biomateriales y Nanomedicina (CIBER-BBN)

[§]Biophysics Group, Department of Physics, Universitat Jaume I, E-12080 Castelló, Spain

[∥]Equipe Physico-chimie de Systèmes Polyphasés, UMR CNRS 8612, Univ Paris-Sud, 92296 Châtenay-Malabry, France

Supporting Information

ABSTRACT: Thermodynamically stable nanovesicle structures are of high interest for academia and industry in a wide variety of application fields, ranging from preparation of nanomaterials to nanomedicine. Here, we show the ability of quaternary ammonium surfactants and sterols to self-assemble, forming stable amphiphilic bimolecular building-blocks with the appropriate structural characteristics to form in aqueous phases, closed bilayers, named quatsomes, with outstanding stability, with time and temperature. The molecular self-assembling of cholesterol and surfactant cetyltrimethylammonium bromide (CTAB) was studied by quasi-elastic light scattering, cryogenic transmission electron microscopy, turbidity (optical density) measurements, and molecular dynamic simulations with atomistic detail, upon varying the cholesterol-to-surfactant molar ratio. As pure species, CTAB forms micelles and insoluble cholesterol forms crystals in water. However, our molecular dynamic simulations reveal that the synergy between CTAB and cholesterol molecules makes them self-assemble into bimolecular amphiphiles and then into bilayers in the presence of water. These bilayers have the same structure of those formed by double-tailed unimolecular amphiphiles.

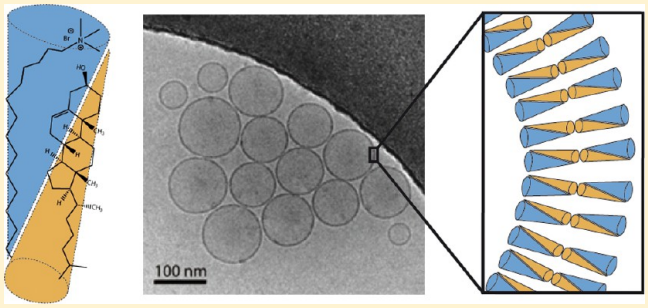

INTRODUCTION

Liposomes made with phospholipids are among the most-studied self-assembled nano-objects since their serendipitous discovery in 1964.[1] They are described as vesicles composed of one or more concentric lipid bilayers, which separate a small enclosed liquid compartment from its surroundings.[2] Their unique structure enables them to trap hydrophobic molecules within their bilayers and hydrophilic molecules within their lumen, making liposomes excellent candidates to be used as nanocarriers for the protection and delivery of active ingredients in pharmaceutical and cosmetic formulations.[3−9] Despite their versatility, the translation to the clinic of liposomal formulations could be hindered by the tendency of these lipid self-assemblies to aggregate and by their low degree of structural homogeneity, which are critical quality attributes with a major impact on the pharmacological properties.[10,11] Liposomes are mostly formed by the input of external energy on a planar lamellar phase (e.g., sonication or mechanical filtration). The stability of these structures is kinetically limited because their lipid building blocks (typically phospholipids or dialkyldimethylammonium halides) are highly insoluble, and therefore, the collapsed planar lamellar is the equilibrium state of aggregation.[12,13] There is a large interest in finding nonlipid building blocks or tectons, which self-assemble into stable vesicles and which satisfy the quality standards required in pharmaceutical formulations.[10,14] For instance, it has been reported that certain amphiphilic polymers, such as block-copolymers, and some polypeptides organize themselves into vesicular-like architectures, giving rise to polymersomes[15−17] and "peptosomes",[18] respectively.[19−21] Other chemical structures such as rod−coil polymers, dendrimers, and amphiphilic fullerene derivatives have also shown to form vesicles.[14]

Spontaneous, single-walled, equilibrium vesicles of controlled size and surface charge can be prepared from aqueous mixtures of cationic and anionic surfactants. Formation of "catanionic vesicles" apparently results from the production of an anion−cation surfactant pair which then acts as a double-tailed zwitterionic surfactant.[22−24]

Nanoscopic vesicles, composed of sterols and quaternary ammonium surfactants, have been prepared by a compressed fluid-based methodology (see the Supporting Information).[25] These vesicular systems, which we named quatsomes, are stable

Received: January 30, 2013
Revised: April 5, 2013
Published: May 6, 2013

   dx.doi.org/10.1021/la4003803 | Langmuir 2013, 29, 6519−6528

for periods as long as several years, their morphologies do not change upon rising temperature or dilution, and they show outstanding vesicle to vesicle homogeneity regarding size, lamellarity, and membrane supramolecular organization.[25,26] These quatsomes have a great potential in the development of new nanomedicines.[27] They have also shown to be effective nanostructures to enhance specific bioactivity of proteins, and to protect them against premature degradation in topical pharmaceutical formulations.[28]

Worth mentioning here is that none of the individual components of a quatsome spontaneously aggregate into vesicular structures, since in water the quaternary ammonium surfactant forms micelles and the insoluble sterol species form crystals. Therefore, the self-assembly of sterol/quaternary ammonium surfactant mixtures into exceptionally homogeneous bilayer vesicles has to be attributed to a synergy between both molecular entities. Understanding the molecular origin and driving force of that synergy is the main concern of this work.

Here, we study at the molecular level the self-assembling of cholesterol and CTAB molecules (Figure 1) in aqueous medium as model components of quatsomes, rationalizing the nature of their exceptional nanostructure. For this purpose, sterol/surfactant mixtures at distinct molar ratios were prepared by sonication in aqueous media. Sonication methodology was chosen among the distinct vesicle preparation routes that avoid any solvent-free stage and are easily handled and commonly used in the literature. Quasi-elastic light scattering (QELS), cryogenic transmission electron microscopy (cryo-TEM), and optical density (OD) were used to characterize the generated supramolecular phases. All-atomic molecular dynamics simulations were used to investigate with atomic resolution the nature of the interactions between the CTAB and cholesterol species in the process of the bilayer formation.

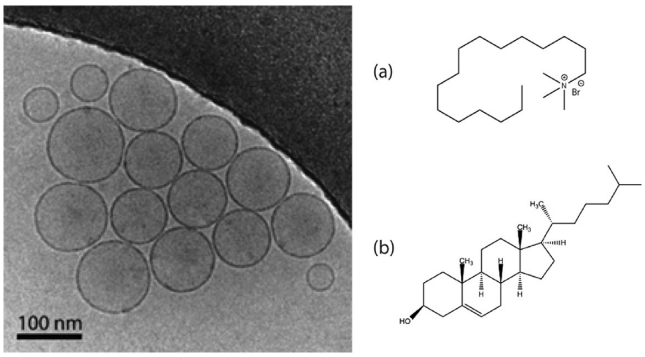

Figure 1. Cryo-TEM image of quatsomes formed by the self-assembling of (a) CTAB and (b) cholesterol molecules.

The pursuit of new building block units able to organize into vesicular structures with improved functionalities such as the ones described in this work is of paramount importance for the development of more efficient drug and gene delivery systems. The technological development of cell mimicking innovative nanocontainers has raised the necessity for understanding the mechanisms of formation and cooperativity behind these self-assembling processes in order to achieve control and predictive capabilities in the bottom-up approach for the fabrication of well-defined nanostructures by rational design.

MATERIALS AND METHODS

Materials. 5-Cholesten-3β-ol (Chol, purity 95%) was obtained from Panreac (Barcelona, Spain). Cetyltrimethylammonium bromide (CTAB, ultra for molecular biology) was purchased from Fluka-Aldrich. Myristyltrimethylammonium bromide (MTAB or cetrimide) was supplied by FeF Chemicals (Koege, Denmark). β-Sitosterol was obtained from Arboris (Savannah, Georgia). All chemicals were used without further purification. The water used was pretreated with the Milli-Q Advantage A10 water purification system (Millipore Ibérica, Madrid, Spain).

Preparation of Chol/CTAB Mixtures by Sonication. Desired amounts of cholesterol and CTAB were weighted in glass bottles and suspended in 10 mL of Milli-Q water (see Table 1). The resulting dispersion was sonicated at 298 K, using a Vibracell Sonifier titanium probe working at 20 kHz (Sonic and Materials Corporation) for 4 min until homogeneous dispersions were achieved. Before analysis, all mixtures were left to stabilize at 298 K for 1 week.

Supramolecular Phases Characterization. *Quasi-Elastic Light Scattering (QELS).* The particle size distribution of the different samples was determined at 298 K using a Zetasizer Nanoseries instrument Nano-ZS (Malvern Instruments, U.K.). It involves a quasi-elastic light scattering (QELS) analyzer combined with a noninvasive backscatter technology (NIBS). The samples (1.0 mL) were measured directly without dilution.

Table 1. Size Distribution of the Supramolecular Aggregates formed by Chol/CTAB Mixtures at Different Molar Ratios in Water Measured by QELS

	size distribution[a]							
	peak 1		peak 2		peak 3		peak 4	
Chol/CTAB molar ratio (Q)[b]	d (nm)[c]	I%[d]	d (nm)[c]	I%[d]	d (nm)[c]	I%[d]	d (nm)[c]	I%[d]
0	1	82	11	5	143	13	–	–
1×10^{-3}	1	27	–	–	157	73	–	–
1×10^{-2}	–	–	–	–	128	100	–	–
0.1	–	–	–	–	119	100	–	–
0.5	–	–	–	–	115	100	–	–
1	–	–	37	21	159	79	–	–
1.5	–	–	20	6	191	90	4144	4
3	–	–	19	6	232	86	5322	8

[a]The size distribution reported is based on intensity of light scattered. [b]Molar ratio between Chol and CTAB (mol/mol) in the system. For all preparations, the CTAB concentration was kept constant above its critical micelle concentration (cmc), at a value of 0.01 M. [c]d is the mean diameter. [d]I% is calculated as the percentage area under the curve.

dx.doi.org/10.1021/la4003803 | *Langmuir* 2013, 29, 6519−6528

Three different experiments were performed in order to check the reproducibility of the results. Results are given in percentage of intensity of scattered light.

Cryogenic Transmission Electron Microscopy (Cryo-TEM). The morphology of the distinct Chol/CTAB assemblies obtained at each Q value was studied by cryogenic transmission electron microscopy using a JEOL JEM-2011 transmission electron microscope (JEOL Ltd., Tokyo, Japan) operating at 120 kV. The samples were frozen by plunge freezing in liquid ethane and stored in liquid nitrogen until loaded onto a cryogenic sample holder (Gatan 626 CTH, Gatan). The working temperature was kept below 98 K. Images were recorded on a Gatan 724 CCD camera under low-dose conditions using Digital Micrograph 3.9.2. (Gatan Inc.).

Optical Density Measurements. The changes in the supramolecular organization of the mixtures as a function of Q were monitored by optical density (OD). The wavelength selected to measure the optical density of the Chol/CTAB systems was λ = 500 nm, at which neither cholesterol nor CTAB absorb.

Molecular Dynamic Simulations. In order to obtain an atomistic view of the self-assembly of CTAB and cholesterol, we have performed all-atomic molecular dynamics (MD) simulations. The MD method is based on the numerical solution of the Newton equations of motion for all atoms of a molecular system constrained to the thermodynamic conditions (T, p, and so forth).

All the MD simulations were performed using the NAMD 2.9 and VMD programs,[29,30] the parameters and protocols of the simulations are described in the Supporting Information.

The model for the molecules was based on the CHARMM22/CMAP force field,[31,32] designed for biomolecular simulations. We used the standard CHARMM force-field parameters for water (TIP3P) and cholesterol, since they are known to correctly predict the solvation free energy of this molecule,[33] a quantity of major importance in the hydrophobic self-assembly processes studied here. The CTAB molecule is composed of a cetyltrimethylammonium cation, modeled following the parameters given in reference 34, and a bromide (Br^-) counterion, modeled employing the parameters given in reference 35.

We have performed simulations of several kinds of systems. First, we have performed bilayer simulations aimed at elucidating the molecular organization of CTAB and cholesterol in vesicles. Since the simulation of a whole vesicle with atomistic detail is impossible with current computer capabilities, we employ the same methodology usually employed to simulate heterogeneous biological membranes containing phospholipids and cholesterol.[36] We consider a bilayer patch in the XY plane in its tensionless state in contact with water maintained at a pressure of 1 in the Z direction (perpendicular to the bilayer). We considered three different bilayers with different compositions, as shown in Table 2.

We have also performed a second kind of simulation (bulk simulation) aimed at elucidating how cholesterol molecules are incorporated inside small micelles of CTAB. In this case (simulation S4 in Table 2), we have considered diluted bulk conditions, that is, a single CTAB micelle with a certain amount of cholesterol molecules inside a large water box. Finally, we have performed several auxiliary simulations of simpler bulk systems which were found to be useful for the interpretation of the results of the previous simulations (simulations A1−A3 in Table 2). In A1, we have considered the simplest possible mixed system, namely one CTAB and one cholesterol molecule in water. In A2, we have considered a small cluster of cholesterol molecules in water. In A3, we have considered a pure CTAB micelle in water.

Table 2. Composition for each Simulation Described in the Text (Number of Molecules of Each Species and Total Number of Atoms) and Equilibrium Size of the Simulation Box (Averaged over Production Runs)

	number of molecules chol./CTAB/water	atoms (total)	Eq box size
S1 (Bilayer)	54/54/5443	23727	15.7 nm^2 × 14.5 nm
S2 (Bilayer)	30/60/5443	22329	11.9 nm^2 × 18.0 nm
S3 (Bilayer)	10/60/5443	20849	14.4 nm^2 × 14.0 nm
S4 (Bulk)	1/72/11109	37937	369.7 nm^3
A1 (Bulk)	1/1/6434	19445	194.0 nm^3
A2 (Bulk)	60/0/1063	7629	70.43 nm^3
A3 (Bulk)	0/72/21176	68064	667.3 nm^3

In some of the previously described simulations, we have computed the Gibbs free energy characterizing self-assembly by employing the adaptive biasing force (ABF) methodology.[29] In these calculations, one starts from the results of the previous, equilibrium MD simulations and obtains the free energy (potential of mean force) over a "reaction" coordinate by applying a biasing force to the system (see the Supporting Information for details).

RESULTS AND DISCUSSION

To investigate the cooperative behavior between cholesterol and CTAB molecules, we have characterized by optical density measurements, quasi-elastic light scattering (QELS), and cryo-TEM the colloidal phases formed in the Chol/CTAB system at different Chol/CTAB molar ratio (Q value). As summarized in Table 1, we have prepared by sonication, different mixtures with Q values comprised between 0 and 3, following the standard procedure described in the experimental section.

The dependence of the optical density at λ = 500 nm with the Q value is shown in Figure 2, together with an image of the nanodispersions. At Q = 0, the dispersed system presents homogeneous and transparent aspect (Figure 2a). The optical density has a value near 0, typical of micelle solutions that do not scatter light at the investigated wavelength. When Q progressively increases from 0 to 1, the dispersion system starts to exhibit a more turbid aspect, which is usual for vesicular and liposomal organizations. Correspondingly, a modest increase in the optical density plot is observed. At Q > 1 solid particles precipitate in the dispersed systems and, consequently, the optical density abruptly increases due to the more intensive light scattering produced by these larger aggregates.

The analysis of each Chol/CTAB mixture by QELS and cryo-TEM (Figures 3 and 4; Figures 2S and 3S of the Supporting Information) evidenced the formation of distinct intermediate supramolecular phases, as suggested in our previous work.[37] In the course of the micelle-to-vesicle-to-crystal transition induced by increasing the cholesterol content in the system, five distinct phase domains can be pictured. Each one governed by a predominant morphology.

In accordance with QELS and cryo-TEM images, the first domain defined at Q = 0 is governed by CTAB micelles with their hydrocarbon core sizing 1 nm (peak 1 in Table 1 and in Figure 3a). Minor populations at 11 and 143 nm (peaks 2 and 3 of Table 1 and Figure 3a) may correspond to larger CTAB

dx.doi.org/10.1021/la4003803 | Langmuir 2013, 29, 6519−6528

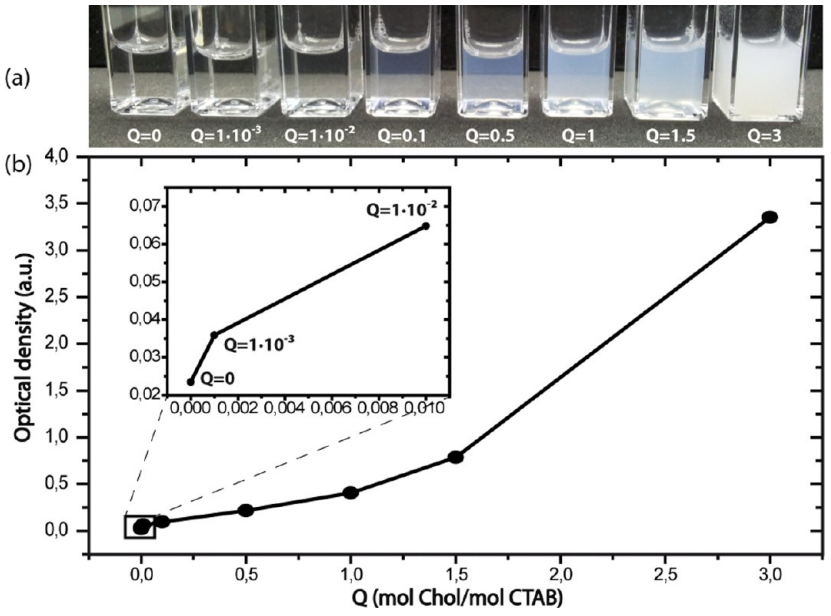

Figure 2. (a) Images of Chol/CTAB mixtures prepared by sonication. (b) Optical density variation, measured at λ = 500 nm, of the self-assembled objects present in Chol/CTAB mixtures in water at different Q values.

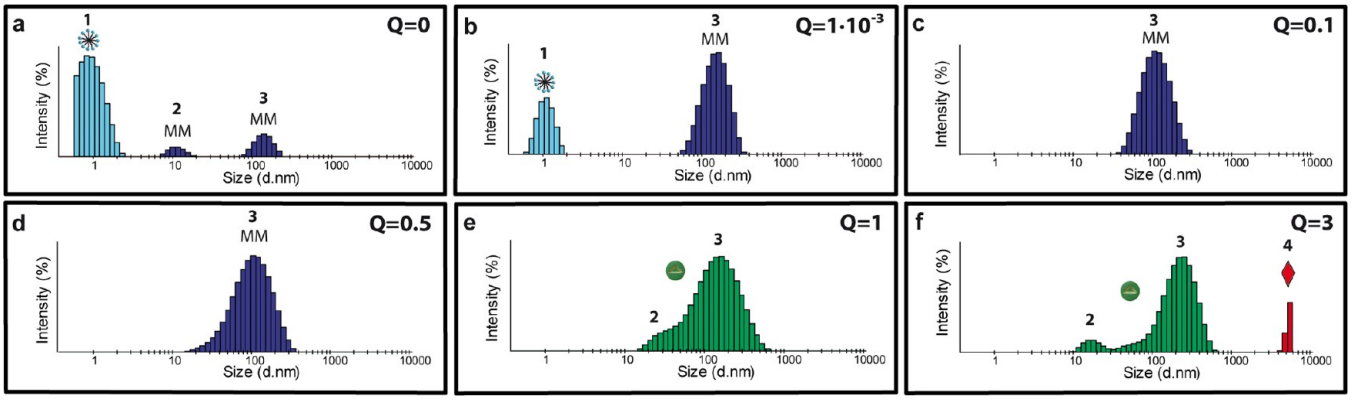

Figure 3. Particle size distributions measured by QELS of supramolecular assemblies present in Chol/CTAB mixtures in water at different Chol/surfactant molar ratios: (a) Q = 0, (b) Q = 1.10^{-3}, (c) Q = 0.1, (d) Q = 0.5, (e) Q = 1, and (f) Q = 3.

micelles or to emergent and unstable CTAB vesicles that we have generically denoted as mixed micelles (MM).[38] As the light scattering intensity (I) in QELS is proportional to d^6, in which d means the particle diameter, even small populations of the 11 and 143 nm sized nano-objects are detected. The second domain comprises Q values between 1 × 10^{-3} and 0.1. At Q = 1 × 10^{-3}, the micellar population (peak 1 of Figure 3b) coexists with a growing population of objects between 70 and 295 nm (peak 3 of Figure 3b). The cryo-TEM images of Figure 4b show the presence of large micelles of elongated flexible shapes also called wormlike micelles (B1). The progressive incorporation of cholesterol to the mixture until Q = 0.1 (Figures 3c and 4c) appears to provoke, according to cryo-TEM, the thickening, folding, and partial self-closing of the worm membrane, generating nascent bilayers (C1). It is reported that above a critical worm size, wormlike micelles tend to curve and self-close in order to minimize their unfavorable edge energies, giving rise to unilamellar vesicles.[19,20,39] On close inspection of Figure 4c, the presence of disklike mixed-micelles (C2) and a closed vesicle (C3) is also revealed. However, statistical analysis of cryo-TEM images confirms the wormlike phase, as the predominant morphology in the second domain. The average size of the colloidal systems generated at Q = 0.1 lies at 119 nm.

The third domain is pictured at Q = 0.5. The cryo-TEM images (Figure 4d) evidenced a change in the primary morphology from worm to disklike mixed micelles (D1) with a particle size mean of 115 nm (Figure 3d). In this domain, disklike micelles coexist with a considerable amount of closed vesicles (D3). Upon addition of cholesterol to the mixture, the destabilizing edge energies of the disklike phase can be minimized either by growth of the floppy bilayers to reduce the overall edge length relative to the membrane area or by bending of the bilayer to form hemisphere caplike structures (D2) with smaller peripheries, which eventually close up on themselves to form vesicles. The equimolar assembling of cholesterol and CTAB (Q = 1) defined the fourth phase domain. At such a molar ratio, the dispersed system contains a pure phase of spherical and unilamellar vesicles (E1 of Figure 4e) with mean diameter sizes around 40 and 160 nm (peaks 2 and 3 of Figure 3e). It is worth saying that these vesicular assemblies are stable for at least 36 months stored at 277 K, and

dx.doi.org/10.1021/la4003803 | Langmuir 2013, 29, 6519−6528

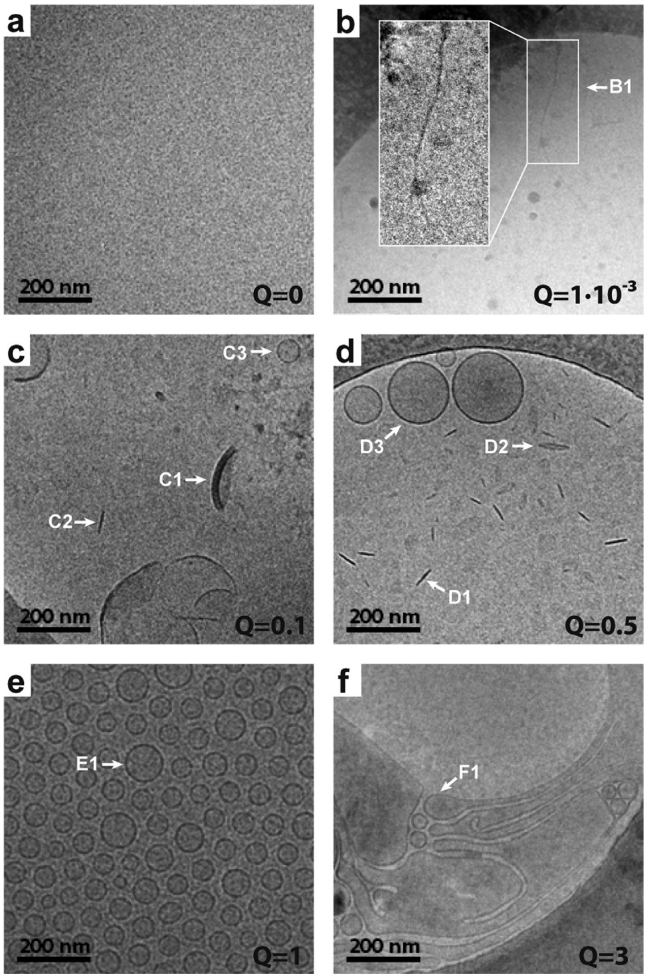

Figure 4. Nanostructures observed by cryo-transmission electron microscopy in aqueous mixtures of Chol and CTAB at different Chol/CTAB molar ratios ranging from 0 to 3: (a) $Q = 0$, (b) $Q = 1 \times 10^{-3}$, (c) $Q = 0.1$, (d) $Q = 0.5$, (e) $Q = 1$, and (f) $Q = 3$. Inset of Figure 4b shows the wormlike micelle aggregates detected at $Q = 1{\cdot}10^{-3}$. B1: worm, C1: nascent bilayer, C2: disk, C3: vesicle; D1: disk, D2: cap, D3: vesicle, E1: vesicle, and F1: distorted vesicle.

they do not change shape upon heating between 298 and 343 K or upon dilution. Finally, the fifth domain is defined at Q values between 1.5 and 3. At such cholesterol/CTAB molar ratio, the smaller number of CTAB molecules compared to the cholesterol ones promotes a macroscopic phase separation between self-assembled nano-objects and platelike cholesterol crystals (solid phase characterization, see the Supporting Information). At $Q = 1.5$, cholesterol crystals (Figures 3S−5S of the Supporting Information) coexist with spherical vesicles but also with elongated and distorted vesicles (F1 of Figure 4f) with diameters ranging between 70 and 460 nm. At $Q = 3$, the phase separation gets more pronounced: the vesicles are more distorted (Figure 4f) and the population of cholesterol crystals in the mixture has dramatically increased (Figure 6S of the Supporting Information). Lafleur et al. have also recently observed the formation of cholesterol crystals in pH-sensitive nonphospholipid vesicular structures composed of stearylamine and cholesterol, when the molar content of cholesterol is larger than that of stearylamine.[40]

To have a molecular picture of the process and the supramolecular structures underlying this transition, we have performed all-atomic molecular dynamics simulations (MD) of mixtures of cholesterol and CTAB in water at the cholesterol/surfactant molar ratios described in Table 2, following the procedures described in the Materials and Methods section.

Let us consider first the conceptually simplest case of a simulation with only one cholesterol and one CTAB molecule in water (simulation A1 of Table 2). The equilibrium state obtained in the simulations corresponds to an association of the cholesterol molecule to the hydrocarbon chain of the surfactant, as can be expected from the hydrophobic character of the sterol unit. The mismatch in size between the two molecular entities and the rigidity of the cholesterol molecule produces a deformation of the polar ammonium headgroup of the surfactant around the polar oxygen group of cholesterol with a separation between N in CTAB and O of the hydroxyl group in cholesterol of 0.58 nm (snapshot of Figure 5). In the

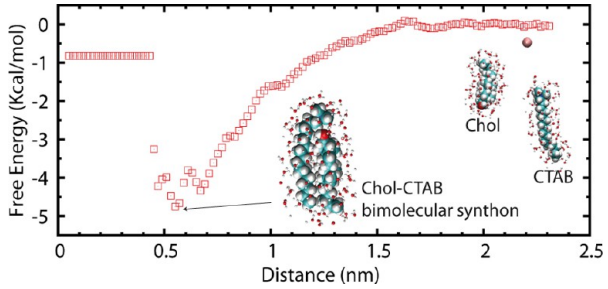

Figure 5. Evolution of the Gibbs free energy of interaction between a single CTAB and a single cholesterol molecule (simulation A1) in water as a function of the intermolecular distance. A snapshot from MD simulations, showing on the right, the initial state of the simulation, and on the left, the structure of the Chol/CTAB supramolecular synthon at the free-energy minimum state.

simulations, we obtain a free energy of $\Delta G = -4.7$ kcal/mol, corresponding to this association (Figure 5). This value for the free energy is large enough to consider that this noncovalent molecular union works as a unique supramolecular synthon or tecton, providing a new building block unit for complex structure formation (snapshot of Figure 5). A simple calculation, based on the classical packing parameter concept,[2,41] suggests that this new supramolecular synthon will form bilayers, as double-chained amphiphiles do. The packing parameter is defined as $f = v/al$, where v is the volume of the hydrocarbon chains of the molecules, l is the length of the hydrocarbon chain, and a is the optimal cross-sectional area per headgroup at the polar hydrocarbon/water interface of the assembly. The necessary condition for the formation of bilayers is $1/2 < f \leq 1$ (see page 299 in ref 2). As seen in the snapshot of Figure 5, the length of the hydrocarbon tail of this supramolecular synthon (l) is approximately that of the cholesterol molecule (1.73 nm) and its volume (v) is approximately the sum of both (0.54 + 0.40 = 0.94 nm^3). The value of a for the synthon can be taken as equal to its value for pure CTAB ($a = 0.64$ nm^2) since the headgroup of the synthon is that of the CTAB surfactant (see again the snapshot of Figure 5). Using these values, we obtain $f = 0.85$, which is consistent with the experimental observation of bilayers at $Q = 1$. Geometrically, this can be easily understood by noting that the CTAB molecule has a conical shape, typical of micelle-forming surfactants ($f = 0.42$ in this case), whereas cholesterol has an inverted conical shape (Figure 6a). The synthon, formed by the assembly of a conical molecule and an inverted conical

dx.doi.org/10.1021/la4003803 | Langmuir 2013, 29, 6519−6528

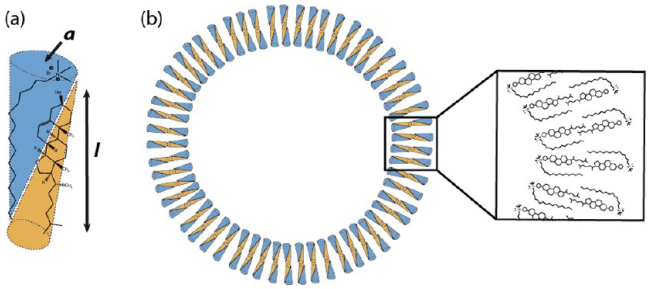

Figure 6. Schematic illustration of the formation of (a) a Chol/CTAB bimolecular amphiphile and (b) their self-assembling into bilayer vesicles based on the packing parameter concept.

molecule, has a cylindrical shape, which is the required shape for the formation of bilayers (see Figure 6b).

The atomistic structure of such a bilayer is investigated in the simulation of a mixture containing equal numbers of CTAB and cholesterol molecules in water (simulation S1 of Table 2). In the simulations (see snapshots of Figure 7a and Figure 11Sa of the Supporting Information), we obtain a homogeneous bilayer in which cholesterol molecules are incorporated in the hydrophobic region of the bilayer (avoiding contact with water) and surfactant molecules are deformed in a way similar to that described in the previous simulation. A more quantitative description of the bilayer structure is given by the atomic density profile, shown in Figure 7a. The headgroup

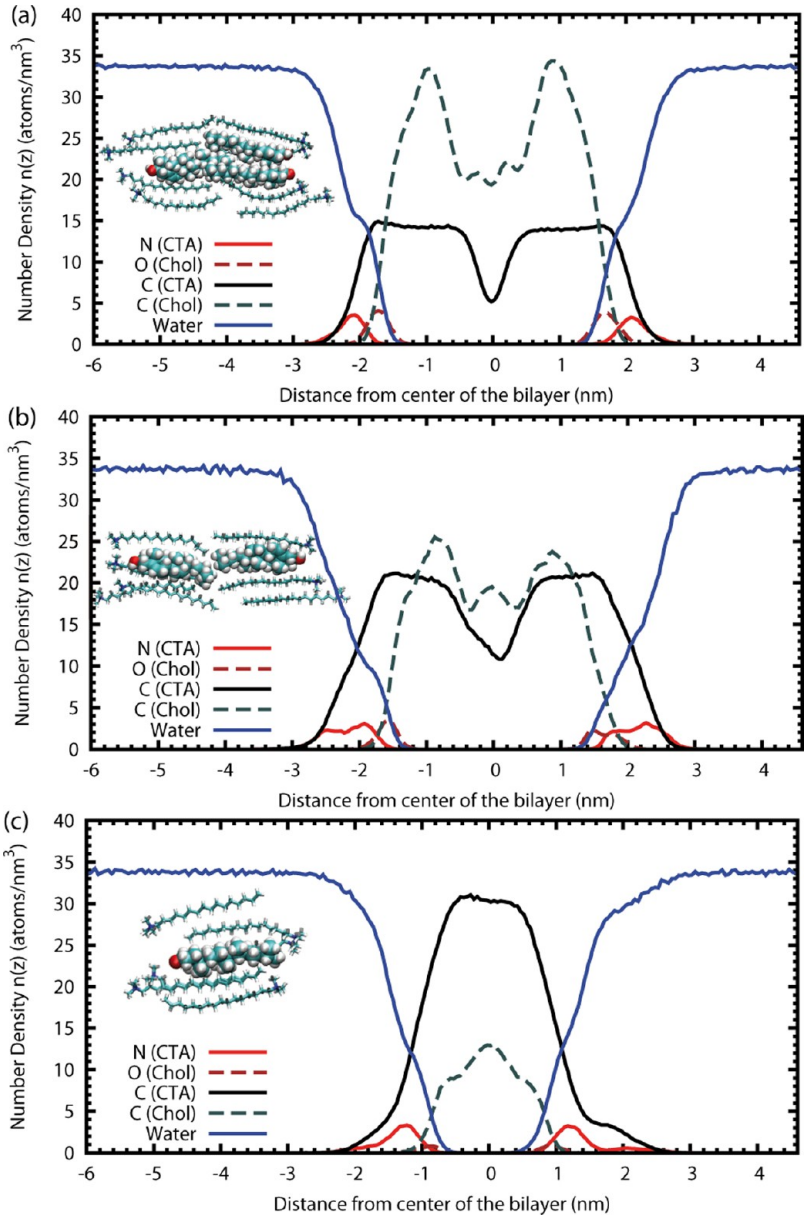

Figure 7. Average density profile of distinct sterol/surfactant mixtures as a function of the z coordinate (perpendicular to the membrane) obtained from MD simulations. (a) S1 ($Q = 1$), (b) S2 ($Q = 0.5$), and (c) S3 ($Q = 0.17$). Solid red line: nitrogen atom from CTAB molecule (atoms/nm^3), dashed red line: oxygen atom from cholesterol molecule (atoms/nm^3), black solid line: carbon atom from CTAB molecule (atoms/nm^3), black dashed line: carbon atom from cholesterol molecule (atoms/nm^3), blue line: water density (molecules/nm^3). Snapshots from MD simulations showing a small portion of the bilayer accompany each atomic density profile (surfactant molecules are shown with bonds-only format, whereas cholesterol molecules are shown using the van der Waals atomic radius).

dx.doi.org/10.1021/la4003803 | *Langmuir* 2013, 29, 6519−6528

and chain distribution of CTAB across the bilayer has the typical shape observed in a two-chain phospholipid bilayer.[42−44] As seen in Figure 7a, the CTAB molecules arrange into two-layered leaflets with the headgroups in contact with water (red lines) and the tails in the interior of the bilayer (black lines). Water molecules (blue line) scarcely penetrate into the bilayer, and the interaction with the membrane components is limited to the solvation of the surfactant polar headgroups. The total bilayer thickness (measured from the peaks in the surfactant headgroup distribution) is about 4.4 nm, and the hydrocarbon region has a thickness about 3.6 nm. These values are in agreement with the average thickness between 4.0 and 5.0 nm, estimated from the cryo-TEM images (see Figure 7S of the Supporting Information). Note also that the atomic distribution of carbon atoms from the surfactant tails has a small density depletion in the center, as observed in typical two-tail phospholipid bilayers (see for example Figure 2 in reference 44). Cholesterol molecules (black lines) accommodate themselves, including the hydroxyl groups (see Figure 7a) in the hydrophobic region generated by the CTAB tails to avoid any contact with the water (blue line) medium. As seen in Figure 7a, the size of this region is enough to accommodate two nonoverlapping layers of cholesterol molecules (note the central minima in the density profile of cholesterol molecules). The cholesterol density profile shows a maximum at 1 nm associated to the overlapping of the rigid carbocyclic moieties of the sterol molecules, as represented in the molecular scheme of Figure 7a. The obtained equilibrium area per polar headgroup is 58 Å^2, similar to that obtained for certain anionic phospholipids [for example, values among 53−55 Å^2 were obtained in MD simulations for anionic phosphatidylserine (PS) lipids].[45,46]

Starting from these MD results, we have performed further ABF−MD simulations (see the Supporting Information) in order to investigate the thermodynamic stability of this bilayer system. Our calculations give ΔG = −35 kcal/mol for the transfer of a surfactant molecule from water to an equimolar bilayer. This quantity has to be compared with the free energy gain of ΔG = −30 kcal/mol for the transfer of a surfactant molecule from water to a CTAB micelle [see flowchart of Figure 13S (e and f) of the Supporting Information]. Similar results are obtained for the cholesterol molecule. We obtain a free energy change of ΔG = −55 kcal/mol for the transfer of a cholesterol molecule into a 1:1 Chol/CTAB bilayer and ΔG = −50 kcal/mol for incorporation into a cholesterol nanocrystal [see flowchart of Figure 13S (b and c) of the Supporting Information]. Therefore, our simulations predict a thermodynamic preference for both CTAB and cholesterol molecules for the mixed environment of an equimolar Chol/CTAB bilayer as compared with a homogeneous environment. The free energy associated with this preference of individual molecules (of about 5 kcal/mol) is almost identical to the binding free energy (4.7 kcal/mol) calculated for the association of a single surfactant with a cholesterol molecule, calculated in simulation A1. Consequently the pair Chol/CTAB works as a unique supramolecular architecture for the formation of more complex colloidal phases, such as vesicles. Overall, all these remarkable structural and thermodynamic properties of a Chol/CTAB bilayer at a 1:1 molar ratio predicted from MD simulations provides theoretical support to justify the experimental high thermal stability (see the Supporting Information) and the exceptional morphological properties attributed to vesicles of such composition obtained following in-solution preparation routes in comparison to vesicles prepared by procedures involving a solvent-free stage.[26]

It is clear that the structure of the bilayer depends crucially on its equimolar composition. In order to understand the dependence with composition, we have performed further simulations of bilayers with different compositions (simulations S2 and S3). The atomic density profiles and snapshots of these simulations [Figure 7 (panels b−c) and Figure 11S (b and c) of the Supporting Information) reveal that the bilayer becomes unstable as the cholesterol/surfactant ratio decreases and suggests the formation of distinct intermediate colloidal phases. In simulation S2 (Q = 0.5), we again observe a bilayer as in the S1 (Q = 1) case. However, the atomic density profiles show a less-defined structure, with a broader distribution of the surfactant headgroups and a decrease in the thickness of the hydrocarbon core of the bilayer (3.2 nm in this case). The accommodation of cholesterol molecules inside the bilayer is now more difficult. There is now a strong overlap of cholesterol in the center of the bilayer, indicated by the unusual central peak of cholesterol in the middle of the bilayer of the atomic density profile (see Figure 7b). The origin of this peak is also evident in the snapshots of Figure 7b and Figure 11Sb of the Supporting Information; it is due to the tail−tail contact between cholesterol molecules located in opposite leaflets. In the case of simulation S3 (Q = 0.17), we obtain a completely different structure. The initial configuration (bilayer) becomes unstable and the system equilibrates at a different structure, made of interdigitated molecules with alternate orientations (see Figure 7c and Figure 11Sc of the Supporting Information). The atomic density profiles no longer have the typical structure of a bilayer. Instead, Figure 7c shows a central hydrophobic region of about 2 nm containing the hydrocarbon tails and the cholesterol molecules and an external hydrophilic region containing the surfactant headgroups and solvation water. Overall, the density profiles of Figure 7c are compatible with the worms and disks morphologies detected by cryo-TEM. However, the exact, supramolecular structure cannot be identified from these simulations due to the unavoidable small size of the simulated system.

Finally, we will briefly discuss how a CTAB micelle is altered by the addition of a small quantity of cholesterol. To this end, we have performed a simulation in which a cholesterol molecule is added to a CTAB micelle in water (simulation S4 of Table 2). The cholesterol molecule is rapidly incorporated into the micelle and protected from water inducing a certain degree of ordering in an inherently disordered micelle (see Figure 12S of the Supporting Information). Starting from these MD simulations, we have also performed ABF calculations in order to determine the free energy involved in the process (see the flowchart of Figure 13Sa of the Supporting Information). We have obtained a free energy of ΔG = −80.8 kcal/mol for the transfer of a cholesterol molecule from water to the micelle, which is more favorable than the transfer from water into a pure cholesterol system (−50 kcal/mol). Therefore, thermodynamics dictate the preferential incorporation of cholesterol into the surfactant micelles.

The transition pathway and transient morphologies induced by the addition of cholesterol to a micellar solution of CTAB observed here are similar to those found in previous studies of the micelle-to-vesicle transition that occurs on mixing cationic and anionic surfactants.[19,47−56] However, the mechanism for which a mixture composed of a cationic surfactant, like CTAB,

dx.doi.org/10.1021/la4003803 | Langmuir 2013, 29, 6519−6528

and a sterol, like cholesterol, self-assemble into a vesicle is rather different and does not have any precedent explanation.

In water, cationic and anionic surfactants individually self-assemble in micelles, but their mixtures are able to self-assemble in more complex structures (including vesicles at nearly equimolar concentrations) due to the electrostatic complexation between cationic and anionic surfactant molecules. In the case of the Chol/CTAB vesicle formation, the self-assembly driving force was not known from previous works. Comparison of the sequence of events described here with the results in mixtures of cationic and anionic surfactants also suggests the complexation between CTAB and cholesterol molecules as the molecular origin for formation of vesicles with improved nanostructure and physicochemical properties. MD simulations confirm that it is the synergy between the CTAB and the sterol entities that generates a bimolecular synthon that at certain proportions behaves as a single building block with adequate structural characteristics to self-assemble into vesicles. This behavior cannot be expected in a heterogeneous mixture of two dissimilar, noninteracting components.[2,55]

In view of these structural results, it is worth emphasizing here the profound, conceptual differences with previous works on transitions from multicomponent membrane vesicles to micelles studied for mixed anionic−cationic surfactants and two-chain lipid systems. In these systems, both molecular types have head groups at the water−hydrocarbon interface.[48] In the mixed cationic−anionic surfactant systems, both polar groups electrostatically interact, modifying the geometry of the system and causing the bilayer and vesicle formation. Instead, in the quatsome system, the sterol does not live at the surface but in the interior of the bilayer (snapshot of Figure 7a). Such particular arrangement of the sterol unit makes the volume of the hydrophobic region of the CTAB molecule apparently increase, leading to the formation of a bimolecular synthon with a structural architecture similar to that of a double-tailed amphiphile, whose spontaneous aggregation geometry is that of a vesicle. Therefore, it is the synergy between one sterol and one single-tail quaternary ammonium surfactant that allows the self-assembling into multicomponent membrane vesicles in aqueous media only at the equimolar proportion that leads to these few repeated structures that we have called quatsomes. These colloidal structures display the required properties to be established as a true thermodynamically stable phase.[22,57]

As reported in the Supporting Information, the same synergy observed for cholesterol and CTAB to form vesicular structures in the aqueous phase has been observed for other equimolar mixtures of quaternary ammonium surfactant and sterols, such as myristyl trimethyl ammonium bromide (MTAB or cetrimide) with cholesterol and CTAB with the plant sterol β-sitosterol.

It is interesting to compare recent simulation results for the behavior of cholesterol inside phospholipid bilayers with that observed in quatsomes. Molecular dynamics simulations employing the coarse-grained MARTINI methodology, which allows the sampling of large time and length scales, have identified a rich phenomenology.[58,59] A flip-flop of cholesterol between the two bilayers[58] can be observed, being faster for unsaturated phospholipids and even a preference for the membrane interior (with an orientation perpendicular to that of the phospholipids) is obtained for polyunsaturated phospholipids.[59] In general, there is no evidence for a possible association between cholesterol and phospholipid molecules. In quatsomes, we expect that cholesterol flip-flop events (which involve the rupture of a cholesterol−surfactant synthon) should be rarer than in phospholipid bilayers. Also, cholesterol mobility inside the quatsomes is expected to be extremely low. Our preliminary results (unpublished) from ongoing large-scale coarse-grained simulations, using the same methodology employed in refs 58 and 59, confirm this view. Again, this simulation supports the exceptional stability with time observed for the Chol/CTAB system in comparison to typical phospholipid formulations (see the Supporting Information). The supramolecular synthon formed by one CTAB and one cholesterol molecule can be considered, to a good extent, as a single entity which self-assembles in particularly stable vesicles, which we called quatsomes.

SUMMARY AND CONCLUSION

Quatsomes are thermodynamically stable vesicular structures, constituted by quaternary ammonium surfactants and sterols. These colloidal structures are stable for periods as long as several years; their morphologies do not change upon rising temperature or dilution and show outstanding vesicle to vesicle homogeneity regarding size, lamellarity, and membrane supramolecular organization. Phase-behavior analysis of different aqueous mixtures of the quaternary ammonium surfactant CTAB and cholesterol, using optical density, quasielastic light scattering, and cryo-TEM, have shown that a pure vesicular phase is only formed at equimolar proportions of both components, whereas coexistence of vesicular structures with other types of colloidal and crystalline phases is observed when one moves away from the equimolar ratio. Molecular dynamic simulations with atomistic detail revealed that the cholesterol and CTAB pair works as a unique supramolecular architecture for the formation of more complex vesicular colloidal phases. This bimolecular synthon can be considered, to a good extent, a single entity which self-assembles in particularly stable vesicles. The remarkable structural and thermodynamic properties of a Chol/CTAB bilayer at a 1:1 molar ratio predicted from MD simulations provide a theoretical support, to justify the experimental high thermal stability and the exceptional morphological properties attributed to vesicles of such composition obtained following in-solution preparation routes in comparison to vesicles prepared by procedures involving a solvent-free stage.

Many functions can be implemented simultaneously in quatsomes, either by covalent attachment to sterol like molecules or by electrostatic interaction with the cationic ammonium head of surfactant units or by hydrophobic interaction with the bilayer. These possibilities open a broad range of applications in pharmacy,[28,60] cosmetics, and materials synthesis.

ASSOCIATED CONTENT

Supporting Information

Preparation and characterization of quatsomes of different compositions by DELOS-susp methodology. Characterization of Chol/CTAB mixtures at molar ratios (Q) of 1×10^{-2}, 1.5, and 3. Membrane thickness determination. Analysis of quatsomes stability with temperature and time. Further details on molecular dynamics simulation methodology and expanded figures. This material is available free of charge via the Internet at http://pubs.acs.org.

AUTHOR INFORMATION

Corresponding Author

*J.F.: e-mail, jfaraudo@icmab.es. N.V.: e-mail, ventosa@icmab.es.

Author Contributions

The manuscript was written through contributions of all authors. All authors have given approval to the final version of the manuscript.

Author Contributions

⊥These authors contributed equally.

Notes

The authors declare no competing financial interest.

ACKNOWLEDGMENTS

This work was supported by grants from DGI, Spain, projects POMAS (CTQ2010-019501), CONSOLIDER-NANOSELECT-CSD2007-00041, FIS2009-13370-C02-02, FIS2010-19810, and to DGR, Catalunya (project 2005SGR00591 and 2009SGR0164). We acknowledge financial support from the Instituto de Salud Carlos III, through "Acciones CIBER". CIBER-BBN is an initiative funded by the VI National R&D&I Plan 2008-2011, Iniciativa Ingenio 2010, Consolider Program, CIBER Actions, and financed by the Instituto de Salud Carlos III with assistance from the European Regional Development Fund. The authors appreciate the financial support through the project "Development of nanomedicines for enzymatic replacement therapy in Fabry disease" granted by the Fundació Marató TV3. E. Moreno-Calvo acknowledges the MICINN for a Juan de la Cierva postdoctoral contract. L.F.-T. thanks the MICINN for her FPI bursary. N.V. thanks Banco de Santander for the chair of Knowledge and Technology Transfer Parc de Recerca UAB-Santander. We also thank TECNIO network for financial support on technological transfer activities related to this work. We also thank the UAB Microscopy service for their help in recording cryo-TEM, TEM, and optical microscopy images. The authors thank the suggestions of Prof. Feral Temelli about the use of sterol components for developing quatsomes.

REFERENCES

(1) Bangham, A. D.; Horne, R. W. Negative staining of phospholipids + their structural modification by-surface active agents as observed in electron microscope. *J. Mol. Biol.* **1964**, *8* (5), 660.

(2) Ninham, B. W; Lo Nostro, P. *Molecular Forces and Self-Assembly in Colloid, Nano Sciences and Biology*, 1st ed.; Cambridge University Press: Cambridge, U.K., 2010.

(3) Gregoriadis, G. Carrier potential of liposomes in biology and medicine 0.1. *New Engl. J. Med.* **1976**, *295* (13), 704−710.

(4) Gregoriadis, G. Engineering liposomes for drug delivery: Progress and problems. *Trends Biotechnol.* **1995**, *13* (12), 527−537.

(5) Lian, T.; Ho, R. J. Y. Trends and developments in liposome drug delivery systems. *J. Pharm. Sci.* **2001**, *90* (6), 667−680.

(6) Malam, Y.; Loizidou, M.; Seifalian, A. M. Liposomes and nanoparticles: Nanosized vehicles for drug delivery in cancer. *Trends Pharmacol. Sci.* **2009**, *30* (11), 592−599.

(7) Sawant, R. R.; Torchilin, V. P. Liposomes as 'smart' pharmaceutical nanocarriers. *Soft Matter* **2010**, *6* (17), 4026−4044.

(8) Whitesides, G. M.; Grzybowski, B. Self-assembly at all scales. *Science* **2002**, *295* (5564), 2418−2421.

(9) Guida, V. Thermodynamics and kinetics of vesicles formation processes. *Adv. Colloid Interface Sci.* **2010**, *161* (1−2), 77−88.

(10) http://ncl.cancer.gov/

(11) Kirby, C.; Clarke, J.; Gregoriadis, G. Effect of the cholesterol content of small unilamellar liposomes on their stability invivo and invitro. *Biochem. J.* **1980**, *186* (2), 591−598.

(12) Dubois, M.; Zemb, T. Phase-behavior and scattering of double-chain surfactants in diluted aqueous-solutions. *Langmuir* **1991**, *7* (7), 1352−1360.

(13) Caboi, F.; Monduzzi, M. Didodecyldimethylammonium bromide vesicles and lamellar liquid crystal. A multinuclear NMR and optical microscopy study. *Langmuir* **1996**, *12* (15), 3548−3556.

(14) Antonietti, M.; Forster, S. Vesicles and liposomes: A self-assembly principle beyond lipids. *Adv. Mater.* **2003**, *15* (16), 1323−1333.

(15) LoPresti, C.; Lomas, H.; Massignani, M.; Smart, T.; Battaglia, G. Polymersomes: Nature inspired nanometer sized compartments. *J. Mater. Chem.* **2009**, *19* (22), 3576−3590.

(16) Discher, B. M.; Won, Y. Y.; Ege, D. S.; Lee, J. C. M.; Bates, F. S.; Discher, D. E.; Hammer, D. A. Polymersomes: Tough vesicles made from diblock copolymers. *Science* **1999**, *284* (5417), 1143−1146.

(17) Zhang, L. F.; Eisenberg, A. Multiple morphologies of crew-cut aggregates of polystyrene-b-poly(acrylic acid) block-copolymers. *Science* **1995**, *268* (5218), 1728−1731.

(18) Kukula, H.; Schlaad, H.; Antonietti, M.; Forster, S. The formation of polymer vesicles or "peptosomes" by polybutadiene-block-poly(L-glutamate)s in dilute aqueous solution. *J. Am. Chem. Soc.* **2002**, *124* (8), 1658−1663.

(19) Shioi, A.; Hatton, T. A. Model for formation and growth of vesicles in mixed anionic/cationic (SOS/CTAB) surfactant systems. *Langmuir* **2002**, *18* (20), 7341−7348.

(20) Xia, Y.; Goldmints, I.; Johnson, P. W.; Hatton, T. A.; Bose, A. Temporal evolution of microstructures in aqueous CTAB/SOS and CTAB/HDBS solutions. *Langmuir* **2002**, *18* (10), 3822−3828.

(21) Jung, H. T.; Lee, S. Y.; Kaler, E. W.; Coldren, B.; Zasadzinski, J. A. Gaussian curvature and the equilibrium among bilayer cylinders, spheres, and discs. *Proc. Natl. Acad. Sci. U.S.A.* **2002**, *99* (24), 15318−15322.

(22) Kaler, E. W.; Herrington, K. L.; Murthy, A. K.; Zasadzinski, J. A. N. Phase-behavior and structures of mixtures of anionic and cationic surfactants. *J. Phys. Chem.* **1992**, *96* (16), 6698−6707.

(23) Marques, E. F. Size and stability of catanionic vesicles: Effects of formation path, sonication, and aging. *Langmuir* **2000**, *16* (11), 4798−4807.

(24) Fukuda, H.; Kawata, K.; Okuda, H.; Regen, S. L. Bilayer-forming ion-pair amphiphiles from single-chain surfactants. *J. Am. Chem. Soc.* **1990**, *112* (4), 1635−1637.

(25) Cano-Sarabia, M.; Ventosa, N.; Sala, S.; Patino, C.; Arranz, R.; Veciana, J. Preparation of uniform rich cholesterol unilamellar nanovesicles using CO_2-expanded solvents. *Langmuir* **2008**, *24* (6), 2433−2437.

(26) Elizondo, E.; Larsen, J.; Hatzakis, N. S.; Cabrera, I.; Bjornhorn, T.; Veciana, J.; Stamou, D.; Ventosa, N. Influence of the preparation route on the supramolecular organization of lipids in a vesicular system. *J. Am. Chem. Soc.* **2012**, *134* (4), 1918−1921.

(27) Elizondo, E.; Veciana, J.; Ventosa, N. Nanostructuring molecular materials as particles and vesicles for drug delivery, using compressed and supercritical fluids. *Nanomedicine* **2012**, *7* (9), 1391−1408.

(28) Ventosa, N.; Cabrera, I.; Veciana, J.; Santana, H.; Martinez, E.; Berlanga, J. A. Vesicles comprising epidermal growth factor and compositions that contain them. *Cuban Patent Appl. CU2012-0112*, 2012.

(29) Phillips, J. C.; Braun, R.; Wang, W.; Gumbart, J.; Tajkhorshid, E.; Villa, E.; Chipot, C.; Skeel, R. D.; Kale, L.; Schulten, K. Scalable molecular dynamics with NAMD. *J. Comput. Chem.* **2005**, *26* (16), 1781−1802.

(30) Humphrey, W.; Dalke, A.; Schulten, K. VMD: Visual molecular dynamics. *J. Mol. Graphics & Modell.* **1996**, *14* (1), 33−38.

(31) MacKerell, A. D.; Bashford, D.; Bellott, M.; Dunbrack, R. L.; Evanseck, J. D.; Field, M. J.; Fischer, S.; Gao, J.; Guo, H.; Ha, S.; Joseph-McCarthy, D.; Kuchnir, L.; Kuczera, K.; Lau, F. T. K.; Mattos, C.; Michnick, S.; Ngo, T.; Nguyen, D. T.; Prodhom, B.; Reiher, W. E.;

Roux, B.; Schlenkrich, M.; Smith, J. C.; Stote, R.; Straub, J.; Watanabe, M.; Wiorkiewicz-Kuczera, J.; Yin, D.; Karplus, M. All-atom empirical potential for molecular modeling and dynamics studies of proteins. *J. Phys. Chem. B* **1998**, *102* (18), 3586−3616.
(32) Mackerell, A. D.; Feig, M.; Brooks, C. L. Extending the treatment of backbone energetics in protein force fields: Limitations of gas-phase quantum mechanics in reproducing protein conformational distributions in molecular dynamics simulations. *J. Comput. Chem.* **2004**, *25* (11), 1400−1415.
(33) Cournia, Z.; Vaiana, A. C.; Ullmann, G. M.; Smith, J. C. Derivation of a molecular mechanics force field for cholesterol. *Pure Appl. Chem.* **2004**, *76* (1), 189−196.
(34) Minisini, B.; Chavand, S.; Barthelery, R.; Tsobnang, F. Calculations of the charge distribution in dodecyltrimethylammonium: A quantum chemical investigation. *J. Mol. Model.* **2010**, *16* (6), 1085−1092.
(35) Lybrand, T. P.; Ghosh, I.; McCammon, J. A. Hydration of chloride and bromide anions - determination of relative free-energy by computer-simulation. *J. Am. Chem. Soc.* **1985**, *107* (25), 7793−7794.
(36) Jo, S.; Lim, J. B.; Klauda, J. B.; Im, W. CHARMM-GUI Membrane Builder for Mixed Bilayers and Its Application to Yeast Membranes. *Biophys. J.* **2009**, *97* (1), 50−58.
(37) Cano-Sarabia, M.; Angelova, A.; Ventosa, N.; Lesieur, S.; Veciana, J. Cholesterol induced CTAB micelle-to-vesicle phase transitions. *J. Colloid Interface Sci.* **2010**, *350* (1), 10−15.
(38) Kuperkar, K.; Abezgauz, L.; Prasad, K.; Bahadur, P. Formation and growth of micelles in dilute aqueous CTAB solutions in the presence of NaNO3 and NaClO3. *J. Surfactants Deterg.* **2010**, *13* (3), 293−303.
(39) Schurtenberger, P.; Mazer, N.; Kanzig, W. Micelle to vesicle transition in aqueous-solutions of bile-salt and lecithin. *J. Phys. Chem.* **1985**, *89* (6), 1042−1049.
(40) Cui, Z. K.; Bouisse, A.; Cottenye, N.; Lafleur, M. Formation of pH-sensitive cationic liposomes from a binary mixture of mono-alkylated primary amine and cholesterol. *Langmuir* **2012**, *28* (38), 13668−13674.
(41) Israelachvili, J. N.; Mitchell, D. J.; Ninham, B. W. Theory of self-assembly of hydrocarbon amphiphiles into micelles and bilayers. *J. Chem. Soc., Faraday Trans. 2* **1976**, *72*, 1525−1568.
(42) Feller, S. E.; Venable, R. M.; Pastor, R. W. Computer simulation of a DPPC phospholipid bilayer: Structural changes as a function of molecular surface area. *Langmuir* **1997**, *13* (24), 6555−6561.
(43) Fennell Evans, D.; Wennerström, H. *The Colloidal Domain: Where Physics, Chemistry, Biology, and Technology Meet*, 2nd ed.; Wiley-VCH: New York, 1999.
(44) Tieleman, D. P.; Marrink, S. J.; Berendsen, H. J. C. A computer perspective of membranes: Molecular dynamics studies of lipid bilayer systems. *Biochim. Biophys. Acta, Rev. Biomembr.* **1997**, *1331* (3), 235−270.
(45) Martin-Molina, A.; Rodriguez-Beas, C.; Faraudo, J. Effect of calcium and magnesium on phosphatidylserine membranes: Experiments and all-atomic simulations. *Biophys. J.* **2012**, *102* (9), 2095−2103.
(46) Martin-Molina, A.; Rodriguez-Beas, C.; Faraudo, J. Charge Reversal in Anionic Liposomes: Experimental Demonstration and Molecular Origin. *Phys. Rev. Lett.* **2010**, *104* (16), 168103−168107.
(47) Weiss, T. M.; Narayanan, T.; Wolf, C.; Gradzielski, M.; Panine, P.; Finet, S.; Helsby, W. I. Dynamics of the self-assembly of unilamellar vesicles. *Phys. Rev. Lett.* **2005**, *94* (3), 038303−038307.
(48) Fattal, D. R.; Andelman, D.; Benshaul, A. The vesicle micelle transition in mixed lipid surfactant systems: A molecular model. *Langmuir* **1995**, *11* (4), 1154−1161.
(49) Fromherz, P. Lipid-vesicle structure: Size control by edge-active agents. *Chem. Phys. Lett.* **1983**, *94* (3), 259−266.
(50) Gradzielski, M. Vesicles and vesicle gels: Structure and dynamics of formation. *J. Phys.: Condens. Matter* **2003**, *15* (19), R655−R697.
(51) Gummel, J.; Sztucki, M.; Narayanan, T.; Gradzielski, M. Concentration dependent pathways in spontaneous self-assembly of unilamellar vesicles. *Soft Matter* **2011**, *7* (12), 5731−5738.
(52) Leng, J.; Egelhaaf, S. U.; Cates, M. E. Kinetics of the micelle-to-vesicle transition: Aqueous lecithin-bile salt mixtures. *Biophys. J.* **2003**, *85* (3), 1624−1646.
(53) O'Connor, A. J.; Hatton, T. A.; Bose, A. Dynamics of micelle-vesicle transitions in aqueous anionic/cationic surfactant mixtures. *Langmuir* **1997**, *13* (26), 6931−6940.
(54) Stuart, M. C. A.; Boekema, E. J. Two distinct mechanisms of vesicle-to-micelle and micelle-to-vesicle transition are mediated by the packing parameter of phospholipid-detergent systems. *Biochim. Biophys. Acta, Biomembr.* **2007**, *1768* (11), 2681−2689.
(55) Podgornik, R. Statistical thermodynamics of surfaces, interfaces, and membranes. *J. Stat. Phys.* **1995**, *78* (3), 1175−1177.
(56) Ollivon, M.; Lesieur, S.; Grabielle-Madelmont, C.; Paternostre, M. Vesicle reconstitution from lipid-detergent mixed micelles. *Biochim. Biophys. Acta, Biomembr.* **2000**, *1508* (1−2), 34−50.
(57) Laughlin, R. G. Equilibrium vesicles: Fact or fiction? *Colloids Surf., A* **1997**, *128* (1−3), 27−38.
(58) Bennett, W. F. D.; MacCallum, J. L.; Hinner, M. J.; Marrink, S. J.; Tieleman, D. P. Molecular view of cholesterol flip-flop and chemical potential in different membrane environments. *J. Am. Chem. Soc.* **2009**, *131* (35), 12714−12720.
(59) Marrink, S. J.; de Vries, A. H.; Harroun, T. A.; Katsaras, J.; Wassall, S. R. Cholesterol shows preference for the interior of polyunsaturated lipid. *J. Am. Chem. Soc.* **2008**, *130* (1), 10−11.
(60) Ventosa, N.; Cabrera, I.; Elizondo, E.; Veciana, J.; Sala, S.; Melgarejo, M.; Royo, M.; Albericio, F.; Pulido, D. Functionalized liposomes for the release of bioactive compounds. *Spanish Patent Appl. P201231020*, 2012.